Broadly wavelength tunable bandpass filters based on long-range surface plasmon polaritons

Jongwon Lee, Feng Lu, and Mikhail A. Belkin*

Department of Electrical and Computer Engineering, The University of Texas at Austin, Austin, Texas 78758, USA
**Corresponding author: mbelkin@ece.utexas.edu*

Received July 5, 2011; revised August 15, 2011; accepted August 26, 2011;
posted August 29, 2011 (Doc. ID 150401); published September 20, 2011

We report a new kind of broadly tunable optical bandpass filters based on unusual properties of long-range surface plasmon polaritons. A 0.004 variation in the refractive index of the dielectric medium translates into 210 nm of bandpass tuning at telecom wavelengths. The tuning mechanism reported here may be used to create compact and widely tunable optical systems and other plasmonic components with broadly tunable optical response. © 2011 Optical Society of America

OCIS codes: 240.6680, 250.5403, 230.7408, 230.7400.

Broad spectral tunability is a desired feature of many photonic and plasmonic components, such as optical filters, semiconductor lasers, and plasmonic materials. The operating principle of compact monolithic photonic filters, such as Mach–Zehnder interferometers, Bragg reflectors, microresonator filters, and distributed feedback lasers, relies on light reflection and interference phenomena [1,2]. As a result, a change in the dielectric constant of a filter medium results in the shift in bandpass wavelength according to the equation

$$\lambda_1/n_1 = \lambda_2/n_2, \tag{1}$$

where λ_1, λ_2 are the two device operating wavelengths that correspond to the two values of the refractive index of the device medium, n_1 and n_2. Since the relative refractive index variation in transparent dielectrics is limited to $\leq 1\%$ for thermo-optic and electro-optic materials and $\leq 15\%$ for liquid crystals, the tuning range of these devices is limited. Optical systems with broader tuning ranges are required for many applications, in particular for various spectroscopic and imaging systems. As a result, a number of approaches to produce optical elements with widely tunable response have been developed using mechanical and micromechanical elements [2,3] and acousto-optic modulation [4] and employing coupled cavities or multisection filters [5–7]. However, all these approaches increase optical system complexity and size.

Here we show that long-range surface plasmon polariton (LR SPP) waveguides may be used to produce simple monolithic optical components in which a given variation of the refractive index of the dielectric cladding material may be translated into any desired filter tuning range. The tuning mechanism reported here may be used to create monolithic bandpass filters with tuning ranges spanning over more than an optical octave, compact and widely tunable diode and quantum cascade laser systems, multispectral imagers, and other plasmonic components with broadly tunable optical response.

The LR SPP is a symmetric TM polarized optical mode that exists in thin (~10–50 nm) metal films embedded in dielectrics with similar refractive indices above (n_t) and below (n_b) the metal [8–11], see Fig. 1(a). Physically, LR SPP originates from coupling of the two surface-plasmon-polaritons waves at the metal/top dielectric and metal/bottom dielectric interfaces to form a low-loss symmetric mode [8–11]. As illustrated in Fig. 1(b), the LR SPP optical mode is well confined and well matched to modes in optical fibers and ridge waveguides [12]. However, as soon as the refractive indices n_t and n_b of the cladding dielectrics are even slightly mismatched, the LR SPP mode first becomes severely distorted (see Fig. 1(c)) and then leaky (see Fig. 2(a)) [9,13–17].

Because of low modal loss, good mode matching to optical modes in fibers, and very simple fabrication steps, LR SPP waveguides have attracted considerable attention recently. A large number of LR SPP-based lightwave devices, including waveguides, couplers, modulators, distributed Bragg reflectors, and optical amplifiers, have been proposed and demonstrated recently [12,18–23]. However, the possibility of using LR SPP modes to create very broadly tunable plasmonic devices that we report here has been unnoticed and unexplored before.

Figure 2(a) shows the calculated LR SPP mode power attenuation, coupling loss, insertion loss, and cutoff point for 5 mm long LR SPP waveguides with different metal stripe width integrated with single-mode optical fibers (SMF-28). We assume $\lambda = 1.55\,\mu$m, $n_b = 1.5$, and $n_t = 1.5 + \delta n$ for the calculations. For numerical calculations, a commercial finite-element package (COMSOL 3.5a) was used to solve the LR SPP mode's complex effective

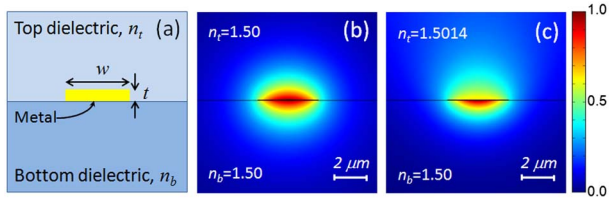

Fig. 1. (Color online) (a) Cross-sectional view of LR SPP waveguide. The metal layer is positioned between top and bottom dielectric layers with refractive indices n_t and n_b, respectively. (b) Calculated intensity profile of a LR SPP mode at $\lambda = 1.55\,\mu$m supported by a 20 nm thick and 4 μm wide gold stripe embedded between loss-less dielectrics with identical refractive indices. (c) Calculated LR SPP mode profile of the same structure with slightly mismatched n_t and n_b.

index n_{eff}. The mode power attenuation was determined from the imaginary parts of the n_{eff}. The total insertion loss was calculated using the power attenuation during the propagation and the LR SPP mode coupling and out-coupling loss at the input and output facets. The coupling/out-coupling loss was evaluated by calculating the overlap integral of the fiber mode (SMF-28) and LR SPP mode. We note that LR SPP mode is the only mode supported by this waveguide [16,20]. As shown in Fig. 2(a), the insertion loss is extremely sensitive to $\delta n = n_t - n_b$. To build a widely tunable bandpass filter out of LR SPP waveguide, we propose using dielectrics with dissimilar refractive index wavelength dispersion as top and bottom cladding. The filter operation is schematically shown in Fig. 2(b). Because of the extreme sensitivity of LR SPP loss on δn, LR SPP mode is only supported at wavelength λ for which $n_t(\lambda) \approx n_b(\lambda)$. A small change in the refractive index of the top dielectric (δn_t) may now be translated into the large shift in the LR SPP filter bandpass ($\delta\lambda$) according to the equation

$$\delta\lambda = \delta n_t / \left(\frac{dn_t}{d\lambda} - \frac{dn_b}{d\lambda} \right), \tag{2}$$

where $dn_t/d\lambda$ and $dn_b/d\lambda$ are the refractive index dispersion of n_t and n_b. Since the value of $(dn_t/d\lambda - dn_b/d\lambda)$ may be controlled by a proper choice of materials (or a combination of materials for composite cladding layers), we can control the tuning range of the filter ($\delta\lambda$) for a given value of δn_t. The bandpass width of the LR SPP filter is determined by the sensitivity of the coupling/propagation loss in the LR SPP waveguides to $\delta n = n_t - n_b$ (see Fig. 2(a)) and the difference in the refractive index dispersions of the top and bottom dielectrics (see Fig. 2(b)).

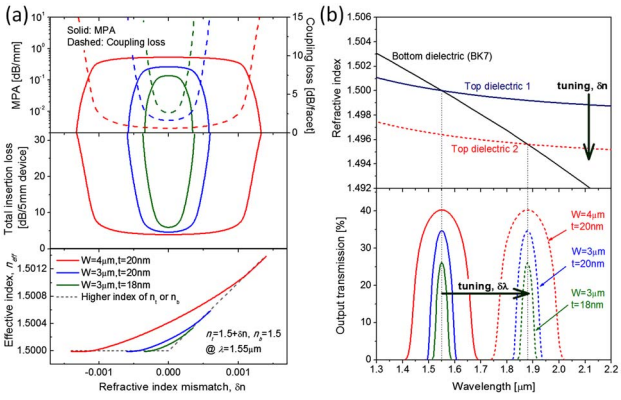

Fig. 2. (Color online) (a) Top: the mode power attenuation (MPA) and coupling loss (per facet) as a function of $\delta n = n_t - n_b$ for LR SPP waveguides with different width (W) and thickness (t) of the Au stripe. Middle: calculation of the total insertion loss for 5 mm long device. Bottom: effective index (n_{eff}) of LR SPP mode as a function δn with different values of W and t. Dashed lines in the figure show the value of the largest of the two cladding indices, n_t or n_b. LR SPP mode becomes leaky when n_{eff} is smaller than the largest of n_t or n_b. (b) Schematic of the LR SPP filter operation. Top: refractive index dispersion curves of the bottom dielectric (BK7 glass) and the refractive-index-tunable top dielectrics. Bottom: calculated optical throughput of the 5 mm long LR SPP filter.

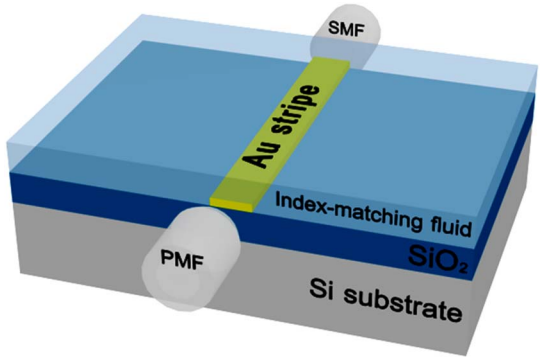

Fig. 3. (Color online) The LR SPP waveguide structure and the experimental configuration. The waveguide was made of 4 μm wide and 20 nm thick stripe of gold on top of a 11 μm thick layer of thermally grown SiO_2 on a silicon substrate. Five types of the refractive-index-matching fluids were used at the top dielectric.

To demonstrate the proposed tuning mechanism experimentally, we operated at near-IR wavelengths ($\lambda = 1.2$–$1.8\,\mu$m) and used a set of five refractive-index-matching fluids as the top dielectric. The experimental configuration is depicted in Fig. 3. The LR SPP waveguide was made of a 4 μm wide 20 nm thick stripe of gold deposited on an optically thick (11 μm thick) layer thermally grown SiO_2 on a silicon substrate. For the experimental demonstration of an LR SPP optical filter, the sample was mounted and covered by refractive index matching fluids. A tunable diode laser ($\lambda =$ 1482 nm–1592 nm) and a broadband source ($\lambda =$ 400 nm–2000 nm) coupled to a polarization-maintaining fiber (PMF) were used to excite the LR SPP mode via end-fire coupling of light. The diode laser was coupled to the PMF to provide TM polarized input to the LR SPP waveguide (as verified by a polarizer); radiation from the broadband source was unpolarized. We note that only TM polarized light can couple to LR SPP. A broadband source was used to obtain data in Fig. 4(b). A brighter diode laser source

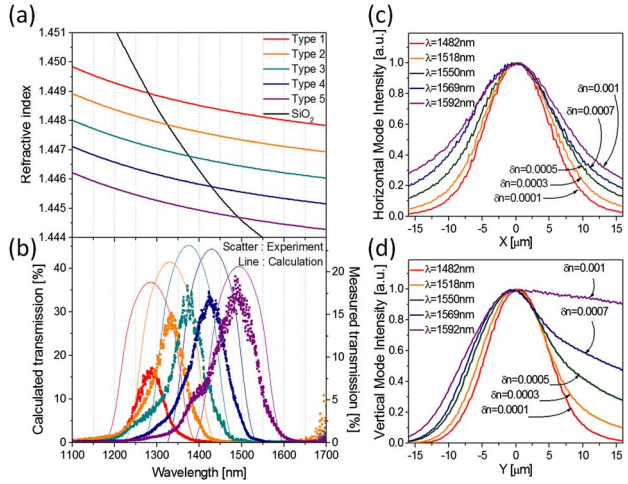

Fig. 4. (Color online) (a) Refractive index dispersion curves for SiO_2 and five different refractive-index-matching fluids (type 1–5) used in experiments. (b) Calculation and experimental results of the filter transmission for the five different types of index matching fluids. (c),(d) Experimental measurements of the horizontal and vertical mode profiles in the LR SPP filter with type five refractive-index-matching fluid at different wavelengths.

was used to obtain the data in Figs. 4(c) and 4(d). The output light was collected by SMF coupled to an optical power meter or optical spectrum analyzer. Both fibers were mounted on a three-axis auto-alignment system. The positions of the input and output fiber were adjusted to maximize the transmitted output power. To obtain transmission spectra of the LR SPP filters, the power spectrum of the LR SPP output was normalized to the power spectrum of the TM polarized component of the input light.

The refractive index dispersion curves for SiO_2 and five different refractive-index-matching fluids are shown in Fig. 4(a). Figure 4(b) shows simulated and experimental power transmission spectra through the 3.1 mm long LR SPP filter. Simulated transmission spectra were calculated using the refractive index dispersion data in Fig. 4(a) and assuming the LR SPP mode is coupled and out-coupled to a SMF. As expected, the filter peak transmission occurs at wavelengths for which $n_t(\lambda) = n_b(\lambda)$; the experimental data of the transmission bandwidth is in good agreement with the theoretical curves. Experimentally, a 0.004 variation in the refractive index of the cladding dielectric translates into 210 nm of bandpass tuning at telecom wavelengths.

Figures 4(c) and 4(d) show measured horizontal and vertical mode profiles in the LR SPP waveguide for different wavelengths of light. In this experiment, type five refractive-index-matching fluid was used as the top cladding dielectric and a tunable diode laser was used as the light source in the end-fire geometry. As expected, the vertical profiles of the LR SPP mode become more distorted as light wavelength moves away from the spectral point at which $n_t = n_b$. At the same time, the horizontal LR SPP mode profiles become slightly broader, maintaining their symmetric shape.

To make practical solid-state filters, one can use thermo-optic materials, electro-optic crystals, or liquid crystal films as the dielectric with tunable refractive index. The bandpass width of the filters may be controlled by changing the design parameters of the LR SPP waveguides to make them more or less sensitive to δn (see Fig. 2(a)). We note that the cutoff point in LR SPP waveguides may be set at an arbitrarily small value of δn by reducing the width and/or thickness of the gold stripe [20]. The bandpass may be narrowed (at the expense of tuning range) by choosing top and bottom dielectric cladding materials with a larger difference in refractive index dispersions [see Eq. (2)]. We note LR SPP filters are expected to operate equally well in the mid-IR spectral range ($\lambda = 3$–$15\,\mu$m), which is very important for chemical sensing and spectroscopy.

In summary, we have demonstrated that LR SPP waveguides may be designed to operate as tunable optical dissipative bandpass filters. The filter design allows one to translate a given refractive index tuning range of the top dielectric cladding into a desired filter bandpass tuning range. The filters are simple in fabrication and may be integrated with fiber-optic and semiconductor laser systems to create optical components with widely tunable spectral response. While it may be difficult to reduce the bandpass of these filters to that of high-fidelity Bragg or microresonator filters, the broad tuning range of these devices is appealing, in particular, for spectroscopic applications and imaging.

This work was supported by the United States Air Force Office of Scientific Research (USAFOSR) under Contract No. FA9550-10-1-0076. Sample fabrication was carried out in the Microelectronics Research Center at the University of Texas at Austin, which is a member of the National Nanotechnology Infrastructure Network. The authors are thankful to professor Ray T. Chen for allowing us to use his laboratory equipment and to Dr. B.S. Lee for demonstrating how to use it.

References

1. G. P. Agrawal, *Lightwave Technology: Components and Devices* (John Wiley & Sons, 2004).
2. O. Solgaard, *Photonic Microsystems* (Springer, 2009).
3. C. Ye, *Tunable External Cavity Diode Lasers* (World Scientific Publishing, 2004).
4. L. Bei, G. I. Dennis, H. M. Miller, T. W. Spaine, and J. W. Carnahan, Prog. Quantum Electron. **28**, 67 (2004).
5. J. W. Evans, J. Opt. Soc. Am. **39**, 229 (1949).
6. I. Šolc, J. Opt. Soc. Am. **55**, 621 (1965).
7. W. T. Tsang, N. A. Olsson, and R. A. Logan, Appl. Phys. Lett. **42**, 650 (1983).
8. M. Fukui, V. So, and R. Normandin, Phys. Status Solidi B **91**, K61 (1979).
9. D. Sarid, Phys. Rev. Lett. **47**, 1927 (1981).
10. H. Dohi, Y. Kuwamura, M. Fukui, and O. Tada, J. Phys. Soc. Jpn. **53**, 2828 (1984).
11. R. Charbonneau, P. Berini, E. Berolo, and E. Lisicka-Shrzek, Opt. Lett. **25**, 844 (2000).
12. J. J. Ju, S. Park, M. Kim, J. T. Kim, S. K. Park, Y. J. Park, and M-H. Lee, Appl. Phys. Lett. **91**, 171117 (2007).
13. L. Wendler and R. Haupt, J. Appl. Phys. **59**, 3289 (1986).
14. J. J. Burke, G. I. Stegeman, and T. Tamir, Phys. Rev. B **33**, 5186 (1986).
15. F. Yang, J. R. Sambles, and G. W. Bradberry, Phys. Rev. B **44**, 5855 (1991).
16. P. Berini, Phys. Rev. B **63**, 125417 (2001).
17. I. Breukelaar and P. Berini, J. Opt. Soc. Am. A **23**, 1971 (2006).
18. G. G. Nenninger, P. Tobiška, J. Homola, and S. S. Yee, Sens. Actuators B **74**, 145 (2001).
19. A. Boltasseva, T. Nikolajsen, K. Leosson, K. Kjaer, M. S. Larsen, and S. I. Bozhevolnyi, J. Lightwave Technol. **23**, 413 (2005).
20. P. Berini, R. Charbonneau, S. Jette-Charbonneau, N. Lahoud, and G. Mattiussi, J. Appl. Phys. **101**, 113114 (2007).
21. S. Jette-Charbonneau and P. Berini, Appl. Phys. Lett. **91**, 181114 (2007).
22. K. Leosson, T. Rosenzveig, P. G. Hermannsson, and A. Boltasseva, Opt. Express **16**, 15546 (2008).
23. I. De Leon and P. Berini, Nat. Photon. **4**, 382 (2010).